

# UV–vis Subpicosecond Spectroscopy of 4-(9-Anthryl)-*N,N'*-dimethylaniline in Polar and Nonpolar Solvents: A Two-Dimensional View of the Photodynamics<sup>†</sup>

Monique M. Martin,\* Pascal Plaza, and Pascale Changenet-Barret

UMR CNRS-ENS 8640 PASTEUR, Département de Chimie, Ecole Normale Supérieure, 24 rue Lhomond, 75231 Paris Cedex 05, France

Aleksander Siemiarczuk

Photon Technology International, 347 Consortium Court, London, Ontario N6E 2S8, Canada

Received: August 8, 2001; In Final Form: November 16, 2001

Transient absorption and gain spectra are reported for 4-(9-anthryl)-*N,N'*-dimethylaniline (ADMA) in polar and nonpolar solvents in the 330–780 nm wavelength range after excitation with a 500-fs laser at 370 nm. In acetonitrile, the initial transient spectra can be interpreted by the superposition of the dimethylaniline cation radical and the anthracene anion radical absorption bands, resulting from the well-known ultrafast photoinduced charge separation. In benzonitrile, similar transient spectra are reached 20–30 ps after excitation. In this solvent, as well as in alcohols, tetrahydrofuran and cyclohexane, the initial UV and visible absorption bands exhibit the spectral characteristics of the locally excited (LE) state. With increasing time, while these bands decay, the signature of the charge-transfer (CT) state appears and one observes a red shift of the region of minimum differential absorption, where gain is expected. These changes occur at a solvent-dependent rate, except in acetonitrile in which the spectra show little evolution because of our limited time resolution. Discrepancies with previously published models for ADMA photodynamics are discussed. In polar solvents except acetonitrile, a quasi-barrierless or slightly activated electron transfer is proposed to explain the long-time decay of the UV absorption band attributed to the LE state. On the other hand, inertial internal torsion around the bond linking the aniline and anthracene moieties in the LE state followed by solvation-induced charge separation similar to that in bianthryl is proposed to explain differences between acetonitrile and benzonitrile or other solvents in the UV range. A two-dimensional picture in which both internal torsion and solvation dynamics determine the excited-state reaction path is discussed, taking into account the initial proposal made by Mataga's group. In cyclohexane, in which solvation effects are not expected, the spectral changes in the picosecond time range are attributed to geometrical relaxation within the  $S_1$  state.

## 1. Introduction

The complex solvent-dependent photodynamics of 4-(9-anthryl)-*N,N'*-dimethylaniline (ADMA, Figure 1) was first reported by Mataga's group in the early seventies<sup>1</sup> and then examined by a number of groups<sup>2–15</sup> within the context of exciplex photophysics, twisted intramolecular charge-transfer (TICT) state<sup>16</sup> formation, and solvent-induced electron-transfer reactions. In early studies, Okada et al.<sup>1,3</sup> demonstrated that the ADMA fluorescence can be attributed to a highly polar charge-transfer (CT) state, involving an electron transfer from the dimethylaniline (DMA) donating group to the anthracene accepting group. They also demonstrated that the radiative lifetime decreases when the solvent polarity increases and invoked a solvent-induced change in the electronic structure of the emissive state. Semiempirical calculations led them to conclude that the locally excited (LE) state is close to the CT state even in low-polarity solvents. Later, from picosecond transient absorption experiments, they concluded that the ADMA photodynamics involves “multiple excited states” with different degrees of charge transfer, solvation, and twist angles between the DMA and anthracene moieties.<sup>8,10</sup>

The question of whether a change in geometry is required for the charge-transfer process to occur was raised<sup>4,5</sup> when the TICT model was proposed to explain the anomalous fluores-

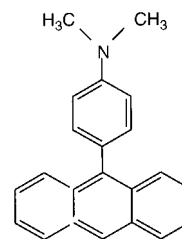


**Figure 1.** Molecular structure of 4-(9-anthryl)-*N,N'*-dimethylaniline (ADMA).

cence of dimethyl-amino-benzonitrile (DMABN) and similar compounds.<sup>4,16</sup> From early quantum chemical calculations, the CT state of ADMA in polar solvents was found to have an equilibrium configuration with orthogonal DMA and anthracene moieties and a polarity-dependent torsional potential shape.<sup>5</sup> It was also found that, in very polar solvents, in its equilibrium 90° twist angle, the CT state lies below the LE state, the torsional potential of which exhibits two minima at flatter configurations.<sup>5</sup> The contribution of a CT transition in the lowest absorption band, as well as the change in conformation and in electronic structure of the CT state depending on the solvent, was also reported for ADMA and several series of analogues.<sup>14,15,17</sup> In these studies, the CT state is also expected to have a flatter configuration in nonpolar solvents than in polar solvents.

<sup>†</sup> Part of the special issue “Noboru Mataga Festschrift”.

In detailed theoretical and femtosecond time-resolved fluorescence studies, Tominaga et al. showed that for ADMA in dimethylformamide (DMF), a very polar solvent, the photodynamics can be well described by a strongly adiabatic electron-transfer reaction involving solvation as the single coordinate.<sup>12,13</sup> The photoinduced CT process was shown to be in the Marcus inverted regime and its kinetics was shown to be composed of two parts: a 150-fs diabatic internal conversion from the  $S_2$  state (mainly of LE character in the Franck–Condon region) to the  $S_1$  state (mainly CT) and an adiabatic, slower, solvent-controlled component on the  $S_1$  surface.<sup>12,13</sup> This model explains the drop of the emission oscillator strength of ADMA in solvents of increasing polarity as well as the time-dependent decrease of the integrated emission intensity in DMF. The experimental observations in polar solvents could thus be explained by neglecting any internal twisting motion in the excited state.<sup>12,13</sup>

Regarding the intrinsic relaxation process in the absence of solvent, a detailed analysis of the laser-induced fluorescence (LIF) spectra of 4-(9-anthryl)-aniline (AA), a nonmethylated ADMA in a supersonic jet, was recently done by Lee et al.<sup>18</sup> It was concluded that for this isolated molecule, the degree of mixing of the LE and CT diabatic states depends on the torsional angle: at equilibrium geometry, with a nonperpendicular configuration, the CT state is lying below the LE state, whereas at the perpendicular position, it is well above the LE state.<sup>18</sup> Both the LE and CT states were indeed found to possess double-minimum potentials with equilibrium angles, respectively, of ca.  $60^\circ$  (and  $120^\circ$ ) and  $50^\circ$  (and  $130^\circ$ ), while the ground state was found to be flexible with a rather flat potential around  $90^\circ$ . A single minimum  $S_0$  and two-minima  $S_1$  torsional potentials were also demonstrated for various 9-phenylanthracene derivatives.<sup>19,20</sup> The determination of the torsional potentials of ADMA in free jet was reported to be difficult because of the congestion of the LIF spectra.<sup>21</sup> Supporting previous claims,<sup>8</sup> Lee et al. proposed that a fully charge-separated state with a perpendicular conformation is expected for ADMA in a polar environment, while a partial charge separation and a smaller twist angle is expected in a less-polar solvent.<sup>18</sup>

To reexamine the ADMA photodynamics in solution, we carried out time-resolved absorption spectroscopy experiments in a variety of solvents at room temperature under subpicosecond excitation at 370 nm. Seven solvents of increasing polarity were tested, from cyclohexane to tetrahydrofuran, alcohols, and nitriles. Femtosecond to picosecond studies of ADMA were generally carried out in polar solvents, and little is known on the excited-state dynamics in a nonpolar solvent. In addition, compared to previous picosecond transient absorption reports,<sup>8,10</sup> the probe spectral range was extended in the UV region down to 330 nm.

## 2. Experimental Section

Time-resolved transient absorption and gain spectra were measured applying the pump–continuum–probe technique using a setup described earlier.<sup>22</sup> The excitation source was a combination of dye lasers<sup>23</sup> pumped by two Nd:YAG lasers and providing 500-fs pulses with 30–40  $\mu\text{J}/\text{pulse}$  around 370 nm. Subpicosecond continuum probe pulses were produced by focusing the laser beam in a water cell. Recording of the pump–probe spectra in the 330–780 nm range was done using a polychromator and a double-diode-array detector. The measurements were carried out at room temperature. The time-resolved spectra were corrected from group velocity dispersion in the probe pulse. The experimental error on the differential optical density ( $\Delta D$ ) is estimated to be  $\pm 0.005$ . The fwhm of the pump–probe temporal response function was fitted to a  $1.0 \pm 0.2$  ps (fwhm) Gaussian.

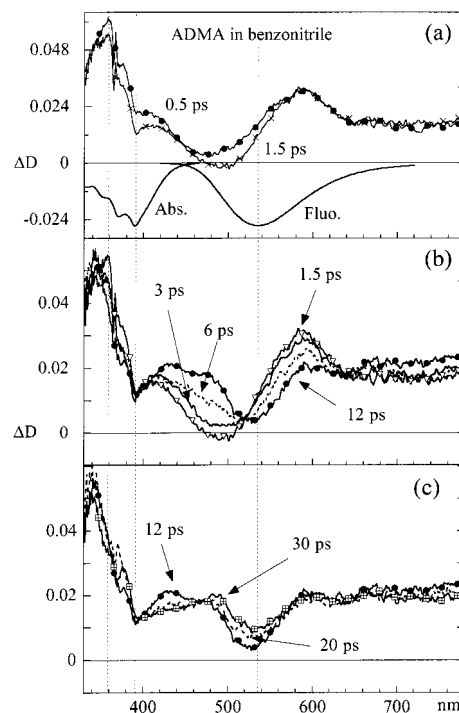


**Figure 2.** Time-resolved differential absorption spectra ( $\Delta D$ ) measured for ADMA in benzonitrile upon subpicosecond excitation at 370 nm for three ranges of pump–probe delays: (a) 0.5–1.5 ps; (b) 1.5–12 ps; (c) 12–30 ps. The normalized ground-state absorption (Abs.) and fluorescence (Fluo.) spectra are shown in panel a to indicate the regions of bleaching and gain.

The ADMA powder was synthesized as previously published.<sup>7</sup> The solutions were prepared with spectroscopy-grade solvents (cyclohexane, tetrahydrofuran, ethanol, 1-propanol, 1-butanol, and acetonitrile from Merck (Uvasol) and benzonitrile from ACROS) without further purification. Only a few milliliters of the solutions was prepared and used in a 1-mm nonrecirculating cell for the pump–probe experiments. The optical density at the excitation wavelength was set between 0.45 and 0.75 depending on the sample. The samples were not deaerated, and it was checked that they were not photolyzing during the experiments by measuring the ground-state absorption spectrum with the pump–probe setup. The steady-state fluorescence spectra were measured with dilute samples and corrected for the fluorometer response function (PTI, QM-2000-04).

## 3. Results

### 3.1. Time-Resolved Spectroscopy in Polar Solvents. 3.1.1.

*Transient Spectra in Nitriles.* Two nitriles were studied: benzonitrile and acetonitrile. Acetonitrile is usually considered as a solvent to be more polar than benzonitrile because of its larger dielectric constant. In terms of other empirical polarity parameters, acetonitrile also has a larger  $E_T^N$  factor<sup>24</sup> than benzonitrile but a smaller  $\pi^*$ .<sup>25</sup> Another difference lies in the solvation time measured from the time-resolved fluorescence Stokes shift of coumarin dyes. The average solvation time in benzonitrile is in the picosecond time range (5.1 ps), whereas that in acetonitrile is in the subpicosecond range (0.26 ps).<sup>26</sup>

3.1.1.1. Benzonitrile. The time-resolved differential absorption spectra ( $\Delta D$ ) measured for ADMA in benzonitrile are shown in Figure 2 for three ranges of pump–probe delays. Both the normalized ground-state absorption and the fluorescence spectra are also shown in Figure 2a to recall the regions where bleaching and stimulated emission are expected to contribute to the observed  $\Delta D$ . Vertical dotted lines are drawn at three wave-

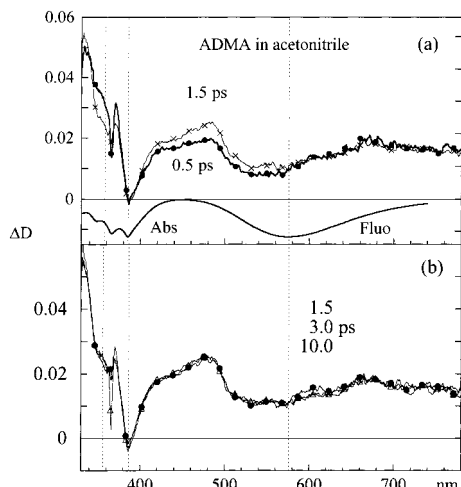


**Figure 3.** Time-resolved differential absorption spectra ( $\Delta D$ ) measured for ADMA in acetonitrile upon subpicosecond excitation at 370 nm for two ranges of pump-probe delays: (a) 0.5–1.5 ps; (b) 1.5–10 ps.

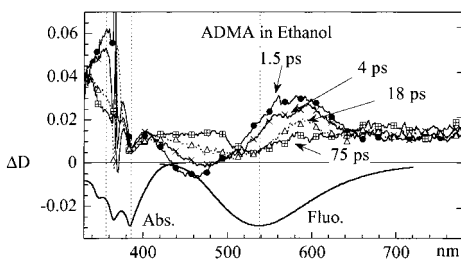


**Figure 4.** Time-resolved differential absorption spectra ( $\Delta D$ ) measured for ADMA in ethanol upon subpicosecond excitation at 370 nm between 1.5 and 75 ps.

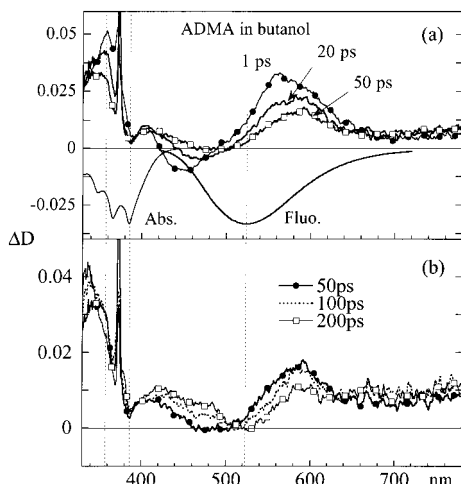


**Figure 5.** Time-resolved differential absorption spectra ( $\Delta D$ ) measured for ADMA in butanol upon subpicosecond excitation at 370 nm for ranges of pump-probe delays below (a) and above (b) 50 ps.

lengths to mark the maxima of the initial UV transient absorption band, the ground-state absorption spectrum, and the fluorescence spectrum. The same presentation is used for other solvents in Figures 3–7. The sharp spikes around 370 nm indicate the region spoiled by scattering of the excitation wavelength. At this wavelength, both the LE and CT states are expected to be excited with, however, a three times larger cross section for the  $S_0 \rightarrow$  LE transition.<sup>12</sup> Immediately after excitation (Figure 2a,  $\Delta t = +0.5$  ps), two broad transient absorption bands are seen with maxima at 358 and 583 nm. In Figure 2a at 0.5 ps, it is seen that  $\Delta D$  is minimum around 475 nm but positive, indicating that stimulated emission, which is expected in this

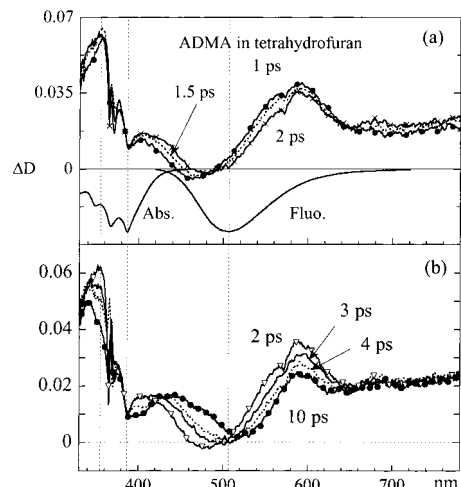


**Figure 6.** Time-resolved differential absorption spectra ( $\Delta D$ ) measured for ADMA in tetrahydrofuran upon subpicosecond excitation at 370 nm for ranges of pump-probe delays below (a) and above (b) 2 ps.

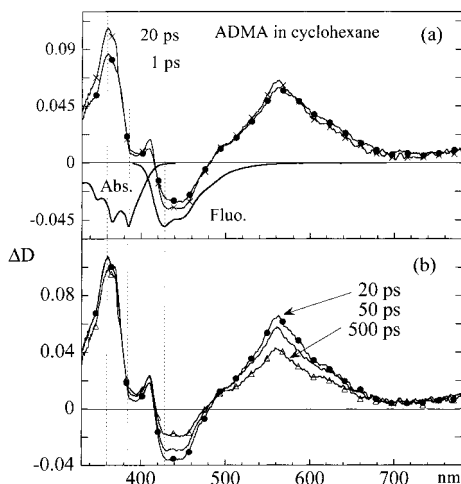


**Figure 7.** Time-resolved differential absorption spectra ( $\Delta D$ ) measured for ADMA in cyclohexane upon subpicosecond excitation at 370 nm for ranges of pump-probe delays below (a) and above (b) 20 ps.

wavelength range, is not dominant. As time increases, between 0.5 and 1.5 ps, one observes a fast decrease of the initial UV band together with the appearance of a dip at 390 nm, at which a bleaching peak is expected. In the same time range, one observes a red shift of the region of minimum  $\Delta D$ , which becomes slightly negative (around 480–500 nm). Further evolution is seen in Figure 2b within 1.5 and 12 ps: the decay of the 358 nm peak is accompanied by an increase of  $\Delta D$  around 340 nm and a red shift of the region of minimum  $\Delta D$  until about 530 nm, the region close to the maximum of the steady-state fluorescence spectrum, and the minimum of  $\Delta D$  becomes positive again. Concomitantly, the 600-nm band decays and the broad and flat absorption band above 650 nm slightly increases. Within this lapse of time, the dip at 390 nm slightly diminishes and regions of roughly constant  $\Delta D$  (nearly temporary isosbestic points) can be seen around 519 and 637 nm. At a 12-ps delay, new absorption maxima appear at 433 and 485 nm. Figure 2c shows that this 400–580 nm region further evolves so that only the 485 nm band remains at 30 ps. Little changes are seen for longer delays. The final transient UV band lies at 340 nm, that is, 18 nm blue shifted from the initial transient band.

3.1.1.2. Acetonitrile. In acetonitrile, the spectrum observed at 1.5 ps (Figure 3a) is similar to that in benzonitrile at 30 ps (Figure 2c), except that the transient absorption around 600 nm

is smaller due to the overlap with the stimulated emission band. As a matter of fact, in acetonitrile, the maximum of the steady-state fluorescence spectrum is 40 nm red shifted from that in benzonitrile. In addition, it must be noted that a tiny negative dip is observed at the maximum of the bleaching band ( $\sim 390$  nm) whereas the region remains positive at all delays in benzonitrile. A fast spectral evolution is seen between 0.5 and 1.5 ps (Figure 3a), characterized by a decay of  $\Delta D$  between 340 and 360 nm together with a rise of a peak below 340 nm and slight change in shape of the transient spectrum between 400 and 580 nm while  $\Delta D$  increases. No further changes in the transient spectra are seen for larger delays (Figure 3b).

### 3.1.2. Transient Spectra in Alcohols and in Tetrahydrofuran.

The transient spectra were measured in ethanol, propanol, and butanol, in which the average solvation time increases, respectively, from 16 to 26 and 63 ps<sup>26</sup> while both the dielectric constant and the  $E_T^N$  factor decrease. The spectral evolution observed in ethanol and in butanol can be seen, respectively, in Figures 4 and 5. The spectral changes are similar to those observed in benzonitrile with a different rate in each solvent. The dynamic shift of the region of minimum  $\Delta D$ , where stimulated emission is expected, slows down when the average solvation time increases from ethanol to propanol and to butanol. One also observes that the initial negative  $\Delta D$  band around 460 nm in ethanol (Figure 4) has a much larger relative amplitude than that in benzonitrile (Figure 2a). This amplitude is still larger in butanol, around 450 nm (Figure 5). The transient spectra recorded in tetrahydrofuran, shown in Figure 6, exhibit the same main features as those observed in nitriles and alcohols except that the absorption band around 480 nm is not well seen at long delay time (Figure 6b), likely because of the overlap with the stimulated emission band. Indeed, the fluorescence maximum is seen around 506 nm in this solvent (Figure 6a). Like in the other polar solvents, the final UV band is blue-shifted compared to the initial one. The negative initial gain band is smaller than that in alcohols. In all cases, for a certain range of delays times, regions of roughly constant  $\Delta D$  (i.e., nearly isosbestic points) are observed around 415–420, 510–520, and 640 nm.

**3.2. Transient Absorption Spectra in a Nonpolar Solvent, Cyclohexane.** The transient absorption spectra recorded for ADMA in cyclohexane are shown in Figure 7, for pump–probe delays shorter and longer than 20 ps, up to 500 ps. From previous analysis of the ground-state absorption spectra in nonpolar solvent or in free-jet spectroscopy, both the LE and CT states are expected to be reached under excitation at 370 nm. The changes shown in Figure 7 are however different from those observed in polar solvents. In Figure 7a, it is seen that after excitation, both the UV peak at 360 nm and the stimulated emission band between 420 and 480 nm keep increasing on the picosecond time range. On the other hand, the visible absorption band exhibits some changes: there is a slight rise of the 560 nm peak and a slight decay of the red side of the band. A detailed analysis of the changes in the stimulated emission band between 0.5 and 4 ps is presented in Figure 8. In Figure 8a, the spectra seem to exhibit an isosbestic point at 421 nm for a negative  $\Delta D$ , at which the ground-state absorption is negligible. The Figure 8b shows the delayed rise of a structure in the stimulated emission band around 430 nm, which is roughly the maximum of the steady-state fluorescence spectrum, together with a decrease of  $\Delta D$  around 390 nm and a rise of the peak at 410 nm. For delays longer than 20 ps (Figure 7b), both the stimulated emission band and the visible absorption band decay with an isosbestic point for a positive  $\Delta D$  at 490 nm. The 360 nm UV peak shows little changes, but an increase

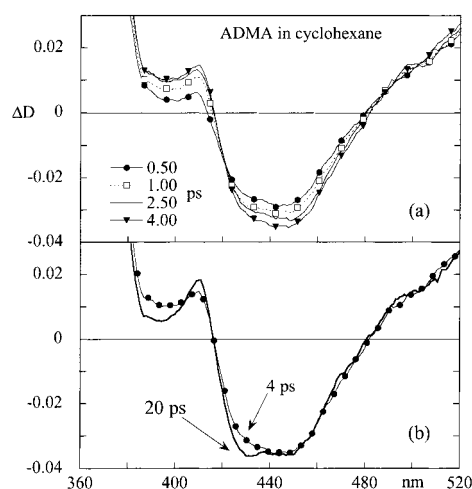


**Figure 8.** Time-resolved differential absorption spectra ( $\Delta D$ ) measured for ADMA in cyclohexane within 4 ps after subpicosecond excitation at 370 nm (a) and between 4 and 20 ps (b) in the spectral region where stimulated emission is observed.

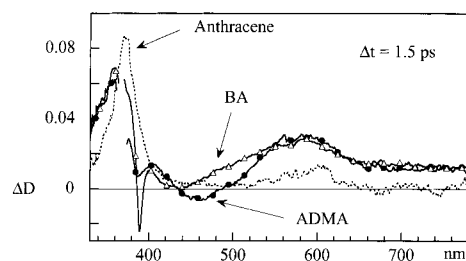


**Figure 9.** Transient absorption spectra of bianthryl<sup>27</sup> and ADMA in ethanol and of anthracene in cyclohexane<sup>27</sup> for a 1.5 ps delay after subpicosecond excitation at 370 nm.

of  $\Delta D$  is observed around 390 nm. The final visible band is in good agreement with the spectrum reported in hexane in previous studies with longer time resolution.<sup>8</sup>

## 4. Discussion

### 4.1. Photoinduced Charge Separation in Polar Solvents.

#### 4.1.1. Interpretation of the Picosecond Time-Resolved Spectra.

**4.1.1.1. Initial Excited State.** In all polar solvents studied here except acetonitrile, the early transient spectra present two absorption bands, one in the UV close to 360 nm and one in the visible around 580 nm. These bands are similar to what we previously reported for bianthryl (BA) in alcohols and in diethyl ether at short times.<sup>27</sup> This can be seen in Figure 9, which shows the transient spectra obtained at 1.5 ps for BA and ADMA in ethanol under similar conditions and of anthracene in cyclohexane. Anthracene exhibits a strong transient absorption band around 370 nm and a much weaker one around 600 nm. Compared to anthracene, BA and ADMA exhibit a relatively stronger band in the visible and a broader and slightly blue-shifted band in the UV. Although one should take into account the contribution of the ground-state bleaching and excited-state stimulated emission to make an accurate comparison of these spectra, one can conclude from Figure 9 that in the excited state of ADMA probed at a 1.5 ps delay, the coupling between the anthracene and dimethylaniline moieties is similar to that observed for the partially torsionally relaxed LE state of BA. As a matter of fact, prior to the spectrum given in Figure 9, we observed an initial fast loss of structure ( $\leq 1$  ps) in the gain spectra of BA, which we attributed to the inertial component of the conformational relaxation within the locally excited LE state<sup>27</sup> from 90° toward 60°. Mataga et al. previously attributed



the initial visible transient spectra of ADMA in butyronitrile and hexanenitrile to the LE state.<sup>10</sup> The present data confirm this attribution. In addition, by comparison with the results that we obtained in BA, we propose that in the LE state an ultrafast inertial rotation of the two moieties with respect to each other leads to an angular distribution of the excited-state population out of the equilibrium ground-state torsion angle, 90°. In benzonitrile, the ultrafast initial decay of the UV band between 0.5 and 1.5 ps, together with the appearance of a dip at 390 nm (Figure 2a) at which a bleaching peak is expected, might result from this rotational motion because one expects the disappearance of the true anthracenic band. The appearance of a dip at 390 nm can be explained by the disappearance of the excited-state absorption, which reveals the overlapped structured bleaching band.

4.1.1.2. Charge-Transfer Reaction. In benzonitrile (Figure 2c), the final transient UV band lies at 340 nm, 18 nm blue shifted from the initial transient band (Figure 2a). As it is close to the spectral limit of our pump-probe setup, 340 nm may not be a true maximum but just the red edge of a transient band extending further in the UV. This final spectrum can be attributed to the solvated CT state. It is indeed known<sup>28</sup> that the radical anion of anthracene possesses a broad absorption band around 330 nm and a less intense absorption region above 550 nm, which is what we see on Figure 2c. The sharp absorption peak expected for the anthracene radical anion around 370 nm is likely to be hidden by scattered light, which spoils the data around the pump wavelength, although such a sharp band was also not observed in differential absorption spectra of 9-methylanthracene in the presence of dimethylaniline.<sup>29</sup> In addition to spectral signatures of the anthracene anion, the characteristic absorption band of the dimethylaniline cation radical is seen around 480 nm.<sup>28</sup> In alcohols and tetrahydrofuran (Figures 4–6), the spectral evolution is similar to that in benzonitrile (Figure 2) with a different rate. It must be noted that the presence of regions of temporary constant  $\Delta D$ , that is, nearly isosbestic points, in the transient spectra indicates that the LE  $\rightarrow$  CT reaction is close to being of the precursor-successor type, which is inconsistent with previous descriptions of the ADMA photodynamics.

Another striking observation is that, in acetonitrile, in which the solvated CT state is observed almost immediately after excitation (Figure 3a), the contribution of the initial excited-state absorption in the bleaching range is much smaller than that in benzonitrile (Figure 2) and in other solvents (Figures 4–6) giving rise to a net negative signal at 390 nm. Taking into account the proposal by Mataga's group that a conformational change of ADMA in the excited-state accompanies the solvation process,<sup>8</sup> one might suggest that in acetonitrile the final transient absorption band (below 330 nm) is narrower than that in the other solvents because of a narrower conformational distribution in the solvated CT state. Following this picture, the remaining transient absorption around 360–400 nm in all other solvents would thus result from a broad distribution of charge-separation degree in the solvated  $S_1$  state.

4.1.2. Dynamic Shift of the Gain Band. From the work of Tominaga et al.,<sup>12</sup> a red shift and a decrease in intensity of the instantaneous fluorescence spectrum are expected for ADMA at a solvation-controlled rate. We thus checked whether the time-resolved shift of the gain region of our spectra can be attributed to solvation. We thus plotted the function  $C(t) = \bar{\nu}_{\min}(t) - \bar{\nu}_{\min}(\infty) / \bar{\nu}_{\min}(0) - \bar{\nu}_{\min}(\infty)$ , where  $\bar{\nu}_{\min}(t)$  is the wavenumber of the  $\Delta D$  minimum at which stimulated emission is expected at time  $t$  (Figure 10). In benzonitrile, the curve can be fitted by a single exponential with a  $4.6 \pm 0.3$  ps time constant, which is in good

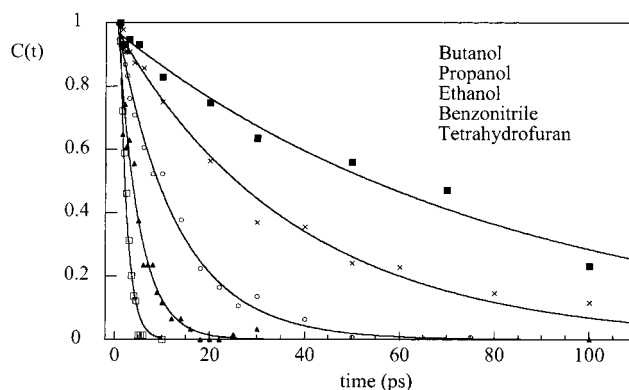


**Figure 10.** Time-resolved shift of the region of minimum  $\Delta D$  observed in the transient absorption spectra of ADMA, where stimulated emission is expected, in different solvents. The shift is expressed by the quantity  $C(t) = \bar{\nu}_{\min}(t) - \bar{\nu}_{\min}(\infty) / \bar{\nu}_{\min}(0) - \bar{\nu}_{\min}(\infty)$  where  $\bar{\nu}_{\min}(t)$  is the wavenumber of the  $\Delta D$  minimum at delay time  $t$ . The experimental results are fitted with a single-exponential function. The fit curve is represented by the continuous line. From left to right, the solvents used are benzonitrile, tetrahydrofuran, ethanol, 1-propanol, and butanol.

agreement with the expected 5.1 ps average solvation time in this solvent.<sup>26</sup> In acetonitrile (Figure 3), in which the average solvation time is as short as 0.26 ps,<sup>26</sup> the gain region is already observed in the region of the steady-state fluorescence immediately after excitation with our 500-fs pump pulse. These trends are in agreement with the results obtained by fluorescence up-conversion methods in dimethylformamide.<sup>12</sup> However, in alcohols, the time constants differ by about 30% with the expected solvation time and in tetrahydrofuran, the  $C(t)$  decay time is twice larger than the average solvation time (Figure 10). The discrepancy is very likely due to the overlap of the stimulated emission and excited-state absorption bands so that the shift of the minimum  $\Delta D$  band does not strictly reproduce that of the stimulated emission band, particularly in the present case in which the gain band is not dominant (Figures 2–6). The reported decrease of the radiative rate accompanying the solvation process<sup>1,12</sup> might contribute to the change in sign of the  $\Delta D$  minimum while shifting (Figures 2 and 4–6). On the other hand, the fact that the radiative rate decreases when the solvent polarity increases<sup>1</sup> might explain the decreasing relative amplitude of the negative gain band observed at short time when the solvent is changed from butanol (Figure 5, 1 ps) to ethanol (Figure 4, 1.5 ps) and benzonitrile (Figure 2, 1.5 ps), although it is much smaller in tetrahydrofuran (Figure 6, 1.5 ps) than in butanol. The relative negative gain amplitude may just be related to the solvation time so that at fixed delay one is probing a different proportion of the LE and CT states.

4.1.3. Kinetic Analysis of the Differential Absorption at Selected Wavelengths. The analysis was carried out at wavelengths at which gain is not expected or is negligible to avoid contribution of the gain-band shift to the kinetics. The differential absorption kinetics,  $\Delta D(t)$ , were analyzed by means of one or two exponentials plus a nanosecond exponential to take into account the excited-state decay previously reported<sup>1,7</sup> but not studied here. The decay kinetics of the initial UV band around 360 nm is shown in Figure 11 in all solvents. In benzonitrile, the decay is also shown at 390 nm at which the contribution of an ultrafast decay component is obvious. In addition to this ultrashort time constant, which falls within our experimental resolution, a second component of  $8 \pm 2$  ps is found for the decay at 357 nm (Figure 11) and of  $8 \pm 1$  ps at 593.5 nm in this solvent. A fit of the decays at the two latter wavelengths with a single exponential leads to values of  $6 \pm 0.5$  ps. If we follow the interpretation of Tominaga et al.,<sup>12</sup> the

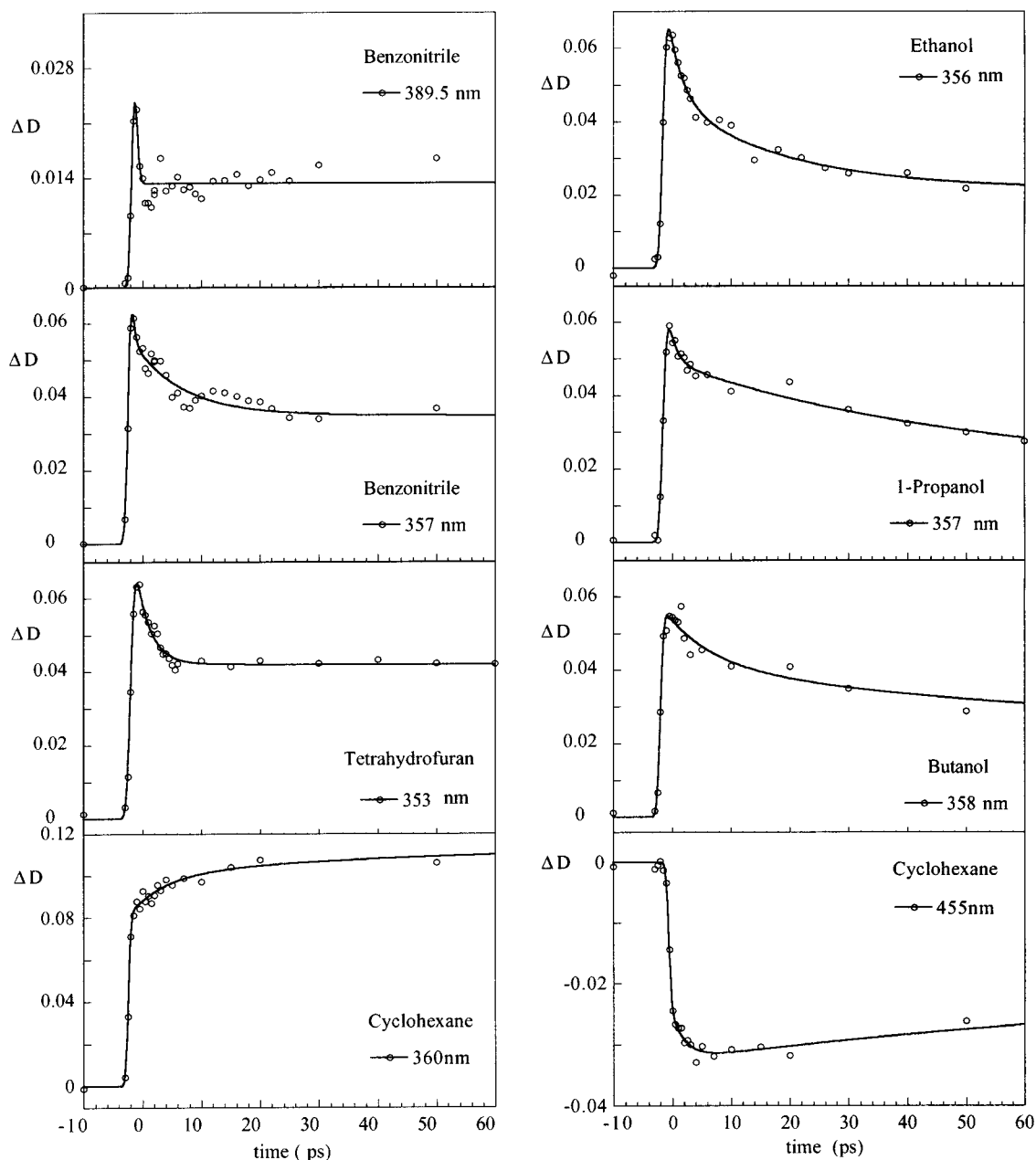


**Figure 11.** Decay or rise kinetics of the initial UV transient absorption band observed for ADMA in different solvents upon excitation at 370 nm. The experimental results are fitted with a one- or two-exponential function plus a nanosecond exponential, which is not seen here. The fit curve is represented by the continuous line.

ultrafast component observed in benzonitrile at 390, 357, and 593 nm, at which the initial LE state is probed, could be due to internal conversion from the  $S_2$  state, of LE character, produced by the pump pulse at 370 nm, to the  $S_1$  state, of CT character, below. It may as well correspond to the escape from the LE character region of the  $S_1$  adiabatic potential. As a matter of fact, in Tominaga's model for ADMA in the very polar dimethylformamide, the LE character vanishes rapidly while the excited-state population propagates on the  $S_1$  barrierless potential along the solvent coordinate and is expected to decrease faster than solvation dynamics.<sup>12,13</sup> However, in benzonitrile, in addition to the ultrashort component, the LE state is found to have a decay component of 8 ps, which is larger than the average solvation time. The average decay time of 6 ps still remains on the order of the solvation time but is not shorter. In dimethylformamide, the reaction was shown to be in the "inverted regime" and barrierless; the LE and CT diabatic states avoided crossing being close to the minimum of the LE state

potential.<sup>12,13</sup> The results that we obtained in acetonitrile may be close to the dimethylformamide case, but the time-resolution of our experiments does not allow us to conclude on the relaxation path. However, in benzonitrile, the 8 ps component indicates the presence of a small barrier on the  $S_1$  potential between the LE and CT states minima, that is, an electron transfer in the "normal regime" so that the reaction can be viewed as a precursor–successor reaction along the solvent coordinate. A slightly activated solvent-controlled LE state  $\rightarrow$  CT state reaction is known for BA in various polar solvents.<sup>27,30</sup> To follow this approach for ADMA, the energy of the CT state, and thus the barrier height between the LE state and CT minima, is expected to be higher in tetrahydrofuran, which is less polar. Indeed, the initial decay kinetics of the UV band at 353 nm (Figure 11) and of the visible band at 600 nm in tetrahydrofuran could be fitted with a single-exponential function, the initial time constants being, respectively,  $2.4 \pm 0.3$  and  $3 \pm 0.3$  ps, which is 2–3 times slower than the solvation time. In alcohols,

the decay of the initial  $\Delta D$  band in the UV at 356–358 nm, attributed to the LE state, can be roughly fitted with two components of 2.5 and 20 ps in ethanol, 1.3 and 50 ps in propanol, and 8 and 75 ps in butanol (Figure 11). The nonexponential character of the decay might be the signature of the nonexponential character of the solvation process because the values fall in the expected time range<sup>26</sup> like that for BA.<sup>27,30</sup>

**4.1.4. Photoinduced Relaxation Path.** The major result of the present experiments is that the initially excited state observed is the LE state in all solvents except acetonitrile. Moreover, its decay kinetics is found to be slightly slower than the solvation process in benzonitrile and tetrahydrofuran or of the same order of magnitude in alcohols. In those solvents, we must invoke a slightly barrier-activated charge separation in the normal region similar to that in bianthryl, which is inconsistent with the model previously proposed for ADMA<sup>12,13</sup> in which the charge-transfer process is in the inverted regime in all solvents and follows an ultrafast LE  $\rightarrow$  CT internal conversion process.

One other important observation of the present study is the difference between the transient spectra of the CT state in the UV range in acetonitrile and in benzonitrile and the other solvents. In section 4.1.1, we suggested to explain this difference by a solvent-dependent distribution of charge-transfer degree in the CT state at equilibrium resulting from a solvent-dependent twist-angle distribution. Along the line of a previously proposed solvation mechanism involving a gradual change in the electronic configuration and geometrical structure<sup>8,10</sup> and to reconcile all observations, we now propose that the reaction occurs on an excited-state surface defined by both the internal twisting and the solvent motion, along a solvent-dependent path. Such a two-dimensional perspective was theoretically developed with success<sup>31</sup> for the photoinduced activated charge-transfer reaction of DMABN in acetonitrile, methanol, and ethanol<sup>32</sup> by Kim and Hynes. In acetonitrile, this model tells that the barrier crossing is mainly along the internal coordinate, whereas in methanol, the solvent coordinate is predominant.<sup>31</sup> Such a two-dimensional model may be needed to describe the ADMA photodynamics in the range of solvent polarity examined here, from the solvent-induced case in highly polar solvents such as dimethylformamide to a path involving both motions in less-polar solvents.

Considering that there is no electronic coupling between the LE and CT diabatic states for a 90° twist angle, we propose that the initial LE state population projected from the orthogonal ground-state population by the excitation pulse evolves quickly toward the 60° equilibrium twist angle on a steep torsion potential, while the solvent is still in the equilibrium configuration around the ground state. This statement implies that the CT and LE state torsional potentials cross for a twist angle close to 90°. This condition is fulfilled when the CT state potential exhibits a single minimum at 90° and is just slightly below the LE state as previously suggested<sup>5</sup> and schematically illustrated in Figure 12a. For a twist angle of 60°, the electronic coupling between the LE and CT diabatic states is nonzero and the CT state is above the LE state. Along the solvent coordinate (defined according to refs 33 and 12), for a 90° twist angle, the diabatic LE and CT states cross in the inverted region (Figure 12b), while for a 60° twist angle, they cross in the normal region (Figure 12c). Considering that the CT state twist angle is 90° at equilibrium, a change in the angular distribution back to 90° is expected in the CT state while the reaction proceeds along the solvent coordinate with a final angular distribution that depends on the torsional potential shape. A two-minima torsional potential is known for the CT state of 4-(9-anthryl)-aniline in the absence of solvent.<sup>18</sup> Such a potential is unfortunately not

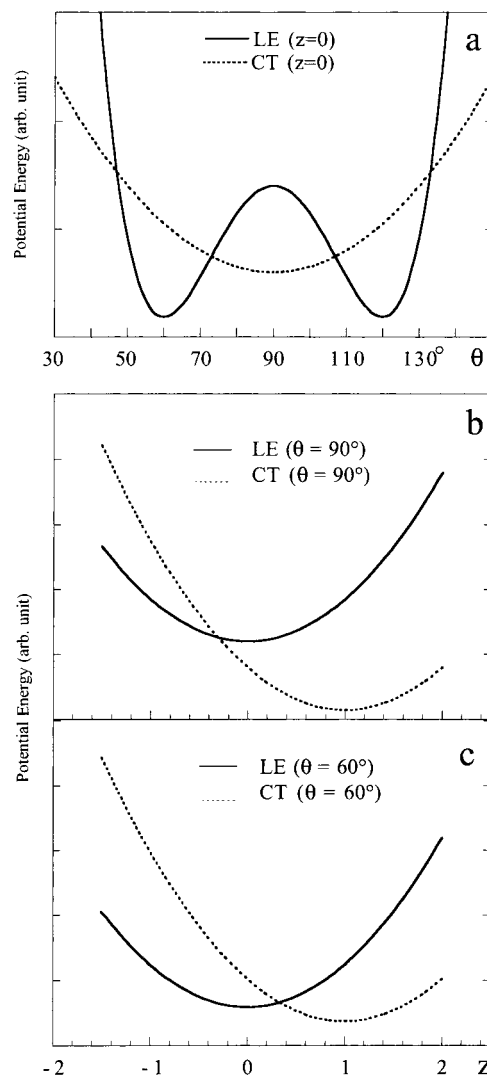


**Figure 12.** Schematic view of the torsional potential of the LE and CT diabatic states for a ground-state equilibrium solvent configuration in a polar solvent (a) and the LE and CT states solvation potentials for a 90° anthracene–dimethylaniline twist angle (b) and for a 60° twist angle (c).

known for ADMA because its determination was reported to be difficult due to the congestion of the LIF spectra.<sup>21</sup> One may however expect a large change in the CT torsional potential shape in solution while solvation proceeds from the initial equilibrium configuration around the ground state to the final equilibrium configuration around the CT state. The resulting path on the excited-state surface may thus strongly depend on the solvent. In particular, one may envisage that the intramolecular coordinate becomes predominant while the solvent polarity decreases as shown by the results obtained in cyclohexane.

**4.2. Photoinduced Structural Rearrangement in Cyclohexane.** In the nonpolar solvent cyclohexane, the main new features observed in the time-resolved spectra (Figures 7 and 8) are the delayed rise of the UV absorption band around 360 nm (Figure 11), the initially observed band in polar solvents, together with the delayed rise and change in shape of the stimulated emission band between 420 and 480 nm (Figure 11). If the temporary isosbestic point observed at 421 nm (Figure 8a) is not fortuitous, it indicates a precursor–successor relationship between two emissive species within a few picoseconds after excitation. Another feature is the decay of both the stimulated emission and the visible absorption bands for delays



longer than 20 ps (Figure 7b) with an isosbestic point at 490 nm indicating further interconverting species. Initial kinetics at selected wavelengths could be fitted with a rising exponential followed by a decaying exponential. The exponential decay time is found to be  $110 \pm 40$  ps at all wavelengths. The rise time component was found to increase with the probe wavelength from 1.6 ps at 560 nm to 2.7 ps at 455 nm, 5.5 ps at 435 nm, and 6 ps at 360 nm.

Considering that solvation is not expected in a nonpolar solvent, one must invoke an intramolecular process to explain the observed changes. As already stressed above, diabatic potentials along the anthracene–aniline torsional angle coordinate were reported to have two-minima for both the LE and CT states in the case of 4-(9-anthryl)-aniline in a supersonic jet with equilibrium angles, respectively, of about  $50^\circ$  (and  $130^\circ$ ) and  $60^\circ$  (and  $120^\circ$ ).<sup>18</sup> Assuming a similar CT potential shape for ADMA, one can imagine that the resulting  $S_1$  adiabatic potential in cyclohexane presents four minima, two of LE character and two of CT character. Taking into account previous claims that the ground-state torsional potential has a flat profile around  $90^\circ$ , one can imagine that the excited-state population produced after excitation at 370 nm is distributed over a large range of torsion angles so that the early spectral changes on a few picoseconds time scale, with time constants depending on the observation wavelength, reflect the propagation of the excited-state population along the  $S_1$  torsional potential toward these minima. The delayed rise of the stimulated emission structure at 435 nm (Figure 8b) and of the UV peak at 360 nm (Figures 7a and 11) indicates that regions of LE character are reached a few picoseconds after those of CT state character. Further equilibrium between the LE and CT populations while the excited molecules are twisting may be at the origin of the 100-ps decay component, the reaction time being determined by the height of the barrier separating the LE and CT minima. Although, further experiments on the subnanosecond time range are needed to conclude on the 100 ps mechanism, the present results clearly demonstrate the existence of an excited-state dynamic process in ADMA in the absence of solvent reorganization.

## 5. Conclusion

In this study, we examined the UV–visible transient absorption and gain spectra of 4-(9-anthryl)-*N,N'*-dimethylaniline (ADMA) upon excitation at 370 nm with a subpicosecond laser in a variety of solvents including cyclohexane. The observations are compared to those previously reported and discussed using the relaxation models proposed by Mataga's group<sup>1,8,10</sup> and Tominaga et al.<sup>12,13</sup> In polar solvents, the initial excited state exhibits the characteristics of the locally excited state except in acetonitrile in which the solvated charge-transfer state is observed immediately after excitation. The LE state is found to decay with kinetics slightly slower than or comparable to the solvation dynamics in the studied solvents, which is not expected from the model of Tominaga et al.. A slightly activated solvent-induced charge separation in the normal region following an ultrafast inertial torsional relaxation in the LE state is proposed to explain the kinetics. In acetonitrile, the UV transient absorption band attributed to the anthracene anion radical is found to be narrower than that in the other solvents and explained by a narrower distribution of the CT-state twist angles between the aniline and anthracene moieties. To try to unify our and others' observations, we propose that the charge-transfer reaction proceeds on an excited state surface defined by the internal twisting and solvent coordinates in a manner similar to what was previously theoretically demonstrated for DMABN<sup>31</sup>

with an increasing contribution of the twisting motion when the solvent polarity decreases. The spectral changes observed in cyclohexane in the picosecond regime demonstrate the existence of an excited-state dynamic process in the absence of solvent reorganization. When we consider the two-minima torsional potentials obtained in the literature for both the locally excited and charge-transfer states of the isolated 4-(9-anthryl)-aniline by Lee et al.,<sup>18</sup> redistribution of the excited population along the  $S_1$  torsional potential is invoked to explain the observations.

**Acknowledgment.** The authors acknowledge financial support from the GDR No. 1017 of the CNRS Department of Chemistry (France). M.M.M., P.P., and P.C.B. thank Prof. J. T. Hynes (UMR CNRS 8640, ENS-Paris France, University Boulder, Colorado, USA) for very helpful discussions during the preparation of this manuscript. M.M.M. also thanks Dr. I. Burghardt (UMR CNRS 8642, ENS-Paris, France) for her help in going through theoretical papers. M.M.M. is very grateful to Prof. N. Mataga for the scientific enrichment that she received from him and served her all along her career.

## References and Notes

- Okada, T.; Fujita, T.; Kubota, M.; Masaki, S.; Mataga, N.; Ide, R.; Sakata, Y.; Misumi, S. *Chem. Phys. Lett.* **1972**, *14*, 563.
- Chandross, E. A. In *The Exciplex*; Gordon, M., Ware, W. R., Eds.; Academic Press Inc.: New York, San Francisco, London, 1975; p 187.
- Okada, T.; Fujita, T.; Mataga, N. *Z. Phys. Chem. N. F.* **1976**, *101*, 57.
- Siemiarz, A.; Grabowski, Z. R.; Krowczynski, A.; Asher, M.; Ottolenghi, M. *Chem. Phys. Lett.* **1977**, *51*, 315.
- Siemiarz, A.; Koput, J.; Pohorille, A. *Z. Naturforsch.* **1982**, *A37*, 598.
- Siemiarz, A. *Chem. Phys. Lett.* **1984**, *110*, 437.
- Siemiarz, A.; Ware, W. R. *J. Phys. Chem.* **1987**, *91*, 3677.
- Okada, T.; Mataga, N.; Baumann, W.; Siemiarz, A. *J. Phys. Chem.* **1987**, *91*, 4490.
- Nagarajan, V.; Brearley, A. M.; Kang, T.-J.; Barbara, P. F. *J. Chem. Phys.* **1987**, *86*, 3183.
- Mataga, N.; Nishikawa, S.; Asahi, T.; Okada, T. *J. Phys. Chem.* **1990**, *94*, 1443.
- Menzel, R.; Windsor, M. W. *Chem. Phys. Lett.* **1991**, *184*, 6.
- Tominaga, K.; Walker, G. C.; Jarzeba, W.; Barbara, P. F. *J. Phys. Chem.* **1991**, *95*, 10475.
- Tominaga, K.; Walker, G. C.; Kang, T. J.; Barbara, P. F.; Fonseca, T. *J. Phys. Chem.* **1991**, *95*, 10485.
- Herbich, J.; Kapturkiewicz, A. *Chem. Phys.* **1991**, *158*, 143.
- Herbich, J.; Kapturkiewicz, A. *Chem. Phys.* **1993**, *170*, 221.
- Grabowski, Z. R.; Rotkiewicz, K.; Siemiarz, A.; Cowley, D. J.; Baumann, W. *Nouv. J. Chim.* **1979**, *3*, 443.
- Herbich, J.; Kapturkiewicz, A. *J. Am. Chem. Soc.* **1998**, *120*, 1014.
- Lee, S.; Kajimoto, O. *J. Phys. Chem. A* **1997**, *101*, 5232.
- Werst, D. W.; Gentry, W. R.; Barbara, P. F. *J. Phys. Chem.* **1985**, *89*, 729.
- Werst, D. W.; Londo, W. F.; Smith, J. L.; Barbara, P. F. *Chem. Phys. Lett.* **1985**, *118*, 367.
- Kajimoto, O.; Hayami, S.; Shizuka, H. *Chem. Phys. Lett.* **1991**, *177*, 219.
- Meyer, Y. H.; Plaza, P. *Chem. Phys.* **1995**, *200*, 235.
- Dai Hung, N.; Plaza, P.; Martin, M. M.; Meyer, Y. H. *Appl. Opt.* **1992**, *31*, 7046.
- Reichardt, C. *Chem. Rev.* **1994**, *94*, 2319.
- Kamlet, M. J.; Abboud, J.-L.; Abraham, M. H.; Taft, R. W. *J. Org. Chem.* **1983**, *48*, 2877.
- Horng, M. L.; Gardecki, J. A.; Papazyan, A.; Maroncelli, M. *J. Phys. Chem.* **1995**, *99*, 17311.
- Jurczok, M.; Plaza, P.; Martin, M. M.; Meyer, Y. H.; Rettig, W. *Chem. Phys.* **2000**, *253*, 339.
- Shida, T. *Electronic absorption spectra of radical ions*; Elsevier: Amsterdam, 1988.
- Nishiyama, K.; Honda, T.; Okada, T. *Acta Phys. Pol.*, **A** **1998**, *94*, 847.
- Kang, T. J.; Jarzeba, W.; Barbara, P. F.; Fonseca, T. *Chem. Phys.* **1990**, *149*, 81.
- Kim, H. J.; Hynes, J. T. *J. Photochem. Photobiol., A: Chem.* **1997**, *105*, 337.
- Changenet, P.; Plaza, P.; Martin, M. M.; Meyer, Y. H. *J. Phys. Chem. A* **1997**, *101*, 8186.
- van der Zwan, G.; Hynes, J. T. *J. Phys. Chem.* **1985**, *89*, 4181.